# Supplement to "Mapping the spatial distribution of $NO_2$ with in situ and remote sensing instruments during the Munich $NO_2$ imaging campaign"

G. Kuhlmann et al.

## S1 Additional Figures

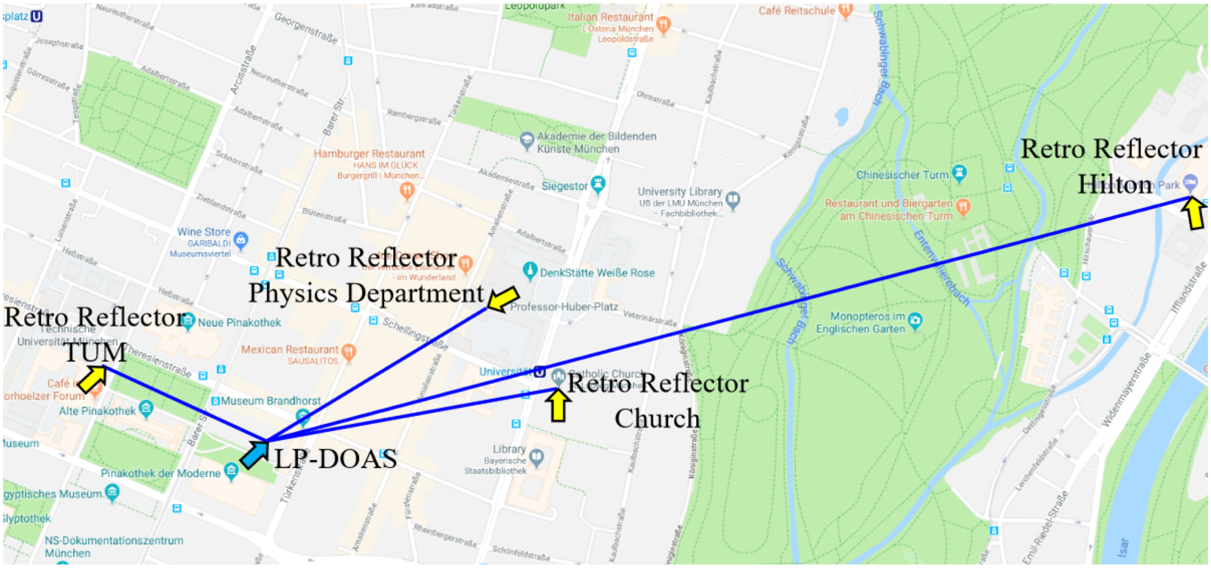


**Figure S1.** The setup of the LP-DOAS system on the MIM's rooftop with its four optical paths towards TUM N5 building, LMU physics building and Hilton hotel (Figure from Zhu et al., 2020). The retro reflector at the Church was only installed in January 2017 and was not available in 2016 during the MuNIC campaign. Map data (c)Google maps.

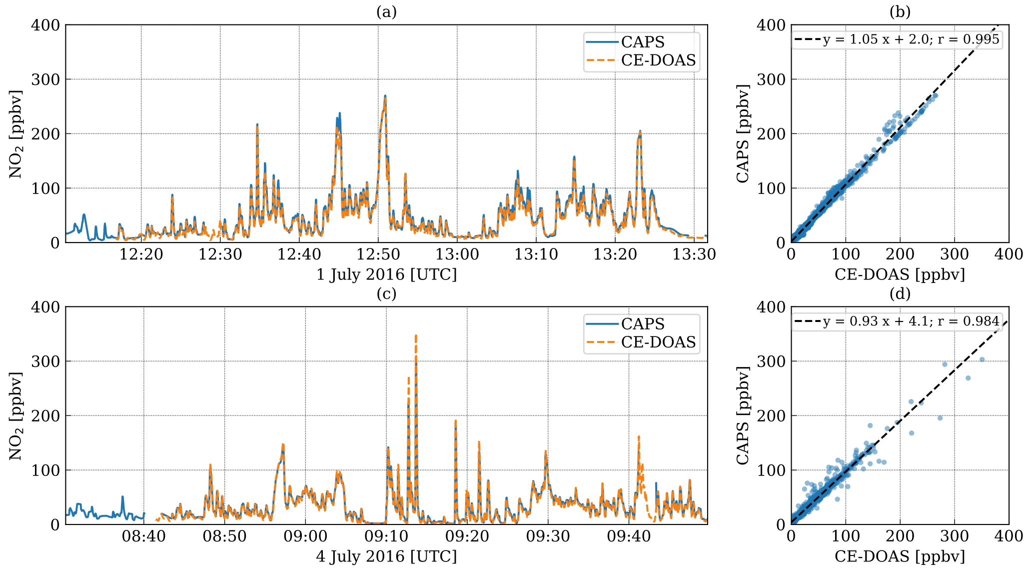


**Figure S2.** (a,c) Time series of $NO_2$ concentrations measured by CAPS and CE-DOAS on 1 and 4 July 2016 on-board the LMU vehicle. (b,c) Scatter plots comparing CAPS and CE-DOAS.

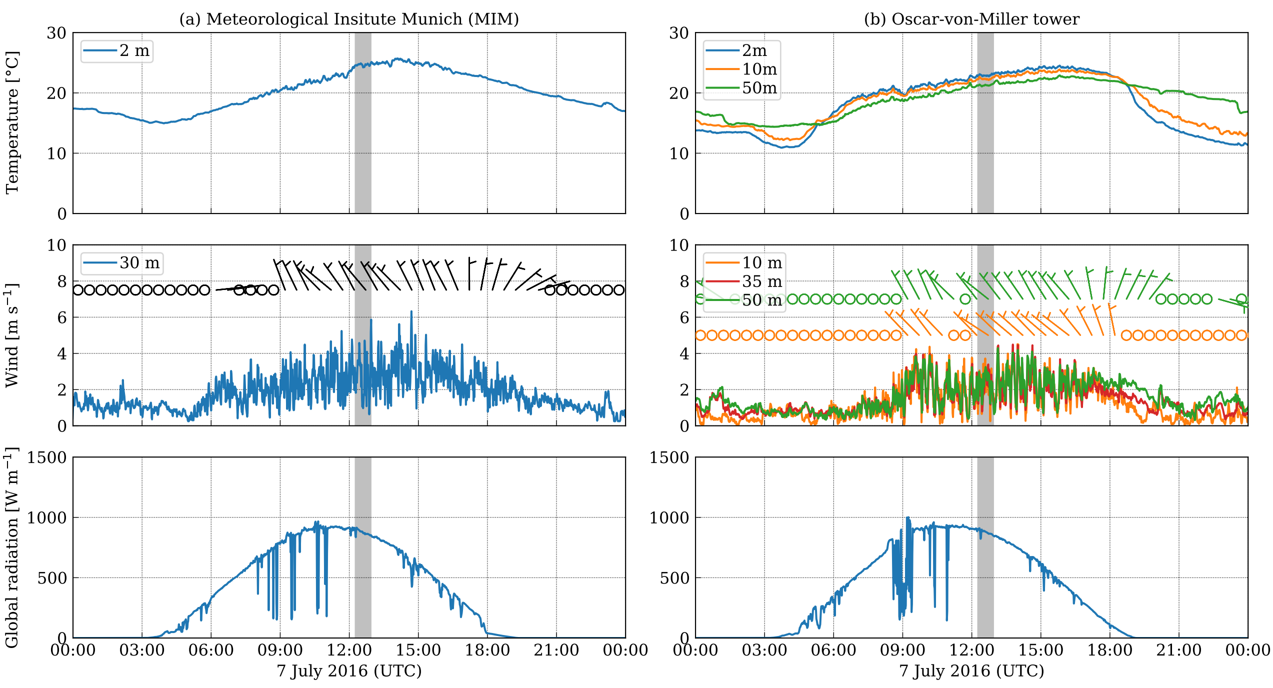


**Figure S3.** Time series of meteorological observations (temperature, wind speed and direction and global radiation) at (a) Meteorological Institute Munich (MIM) and (b) at the Oscar-von-Miller (OvM) tower. The APEX flight time is shown as gray area.

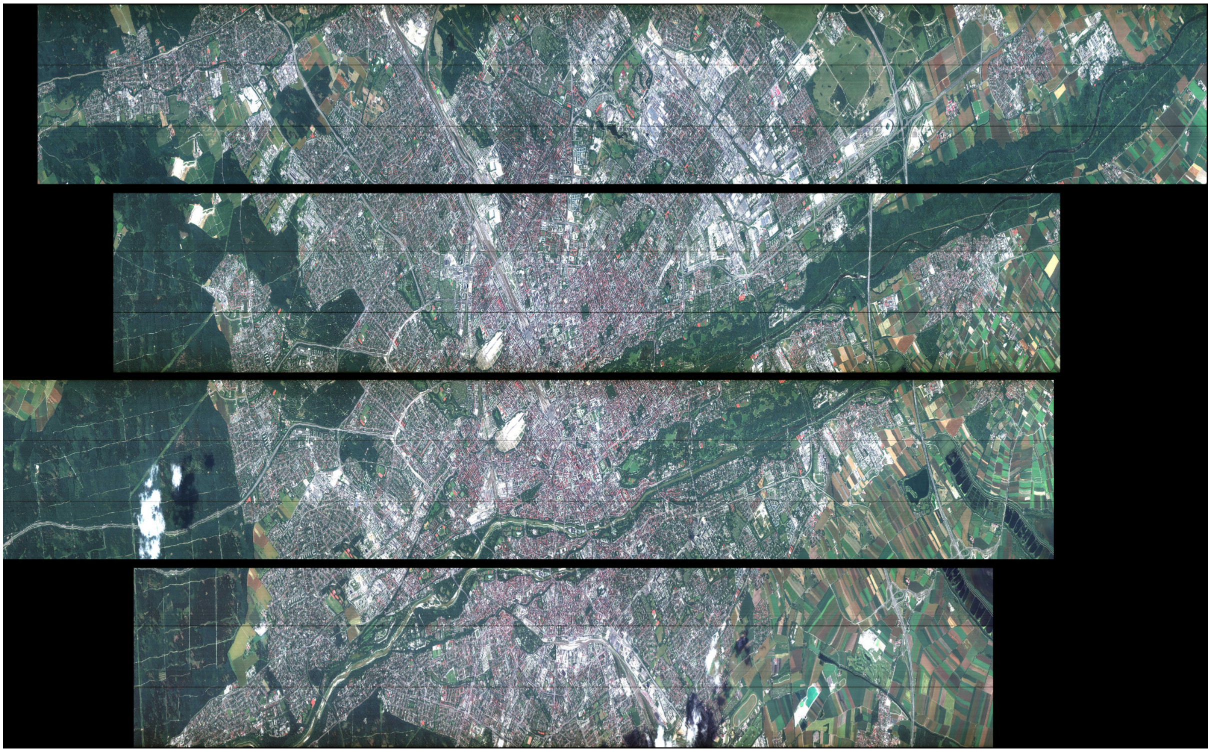

**Figure S4.** True color composite of the four APEX stripes (#1 to #4 from bottom to top) measured during the MuNIC campaign.

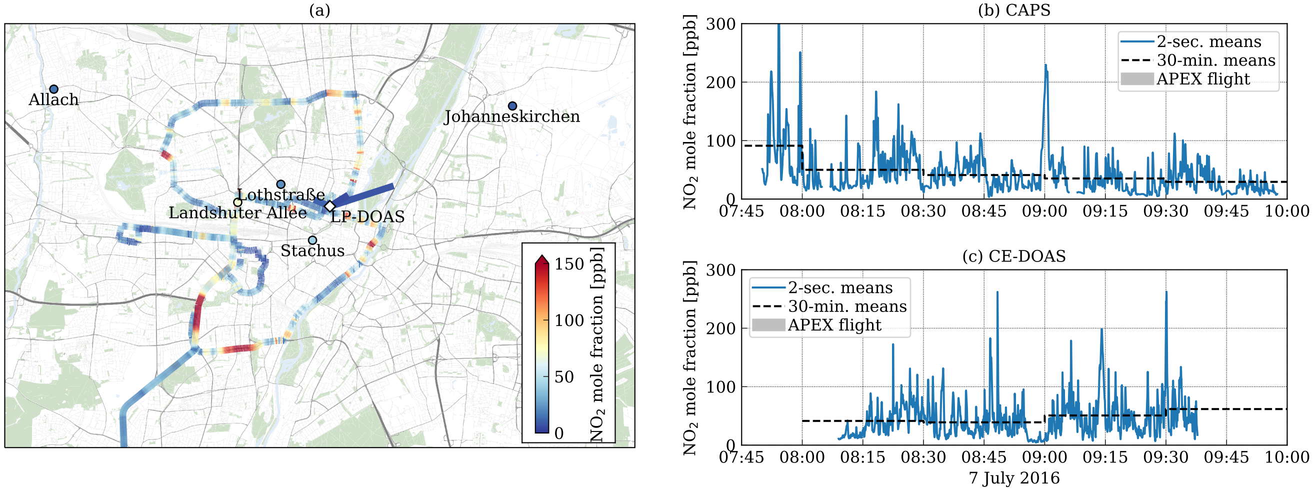


**Figure S5.** (a) Map of $NO_2$ mole fractions measured by LMU and MPIC cars in the morning. (b) and (c) show the time series of $NO_2$ mole fractions measured by the CAPS and CE-DOAS instrument on the LMU and MPIC car, respectively. Map data from © OpenStreetMap contributors 2021. Distributed under the Open Data Commons Open Database License (ODbL) v1.0.

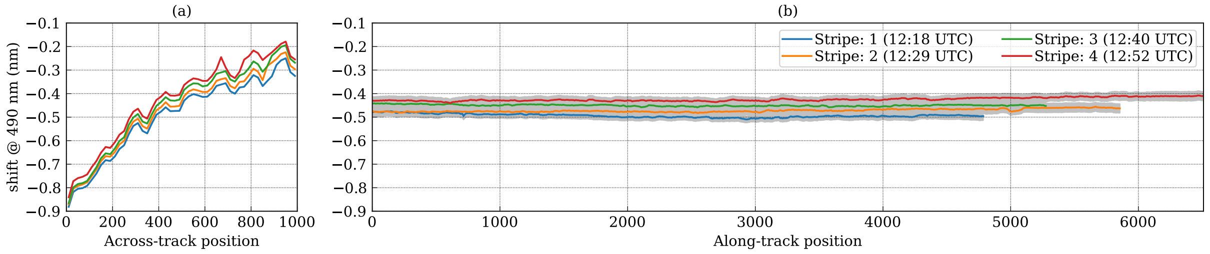


**Figure S6.** Mean (a) across- and (b) along-track shift of center wavelength at 490 nm after in-flight calibration for the four APEX stripes. Gray area shows standard error for all across- and along-track pixels.

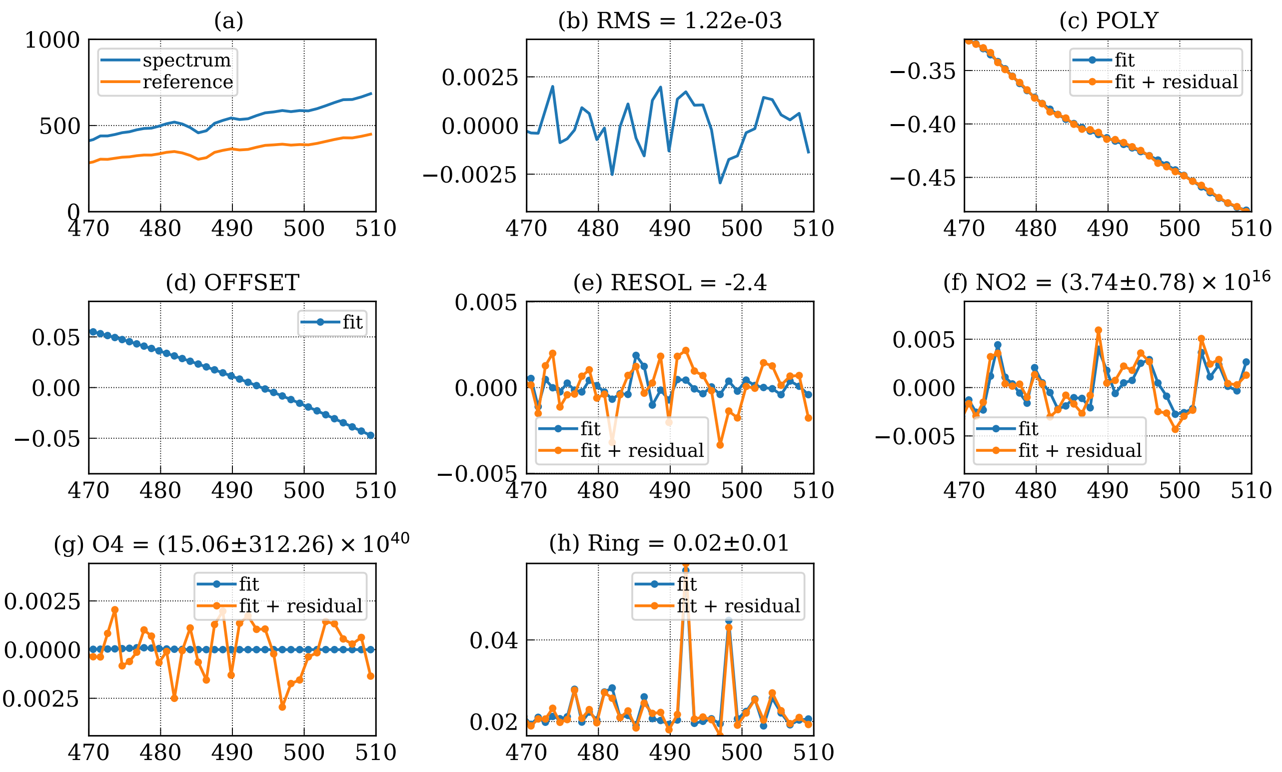


**Figure S7.** Example for DOAS retrieval for APEX Stripe #2 inside the $NO_2$ plume of the Heizkraftwerk Süd power plant at across and along-track positions of 42 and 314, respectively: (a) APEX measurement spectrum and reference spectrum, (b) residual, (c) fitted polynomial, (d) fitted offset, (e) resolution cross section, (f) $NO_2$ cross section, (g) $O_4$ cross section and (h) Ring pseudo cross section.

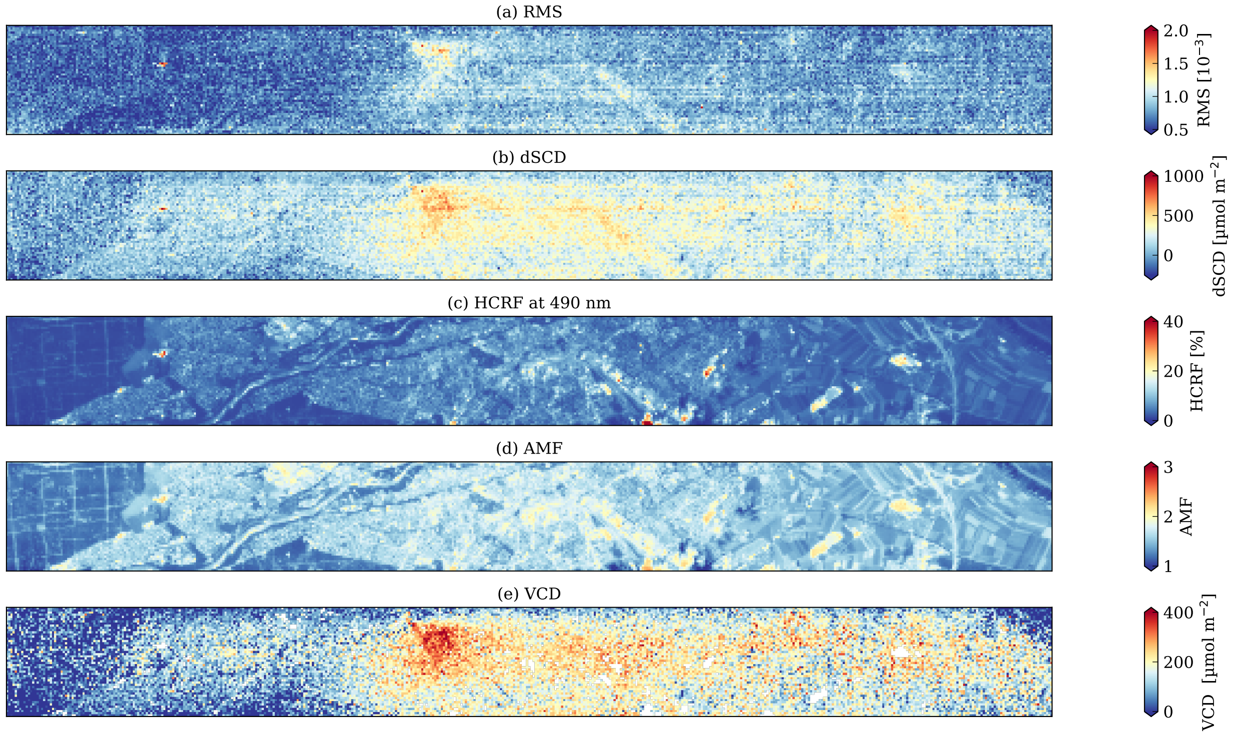


**Figure S8.** APEX stripe #1: (a) root mean square errors (RMS), (b) $NO_2$ differential slant column densities (dSCD), (c) surface reflectance, (d) air mass factors (AMF) and (e) $NO_2$ vertical column densities (VCD).

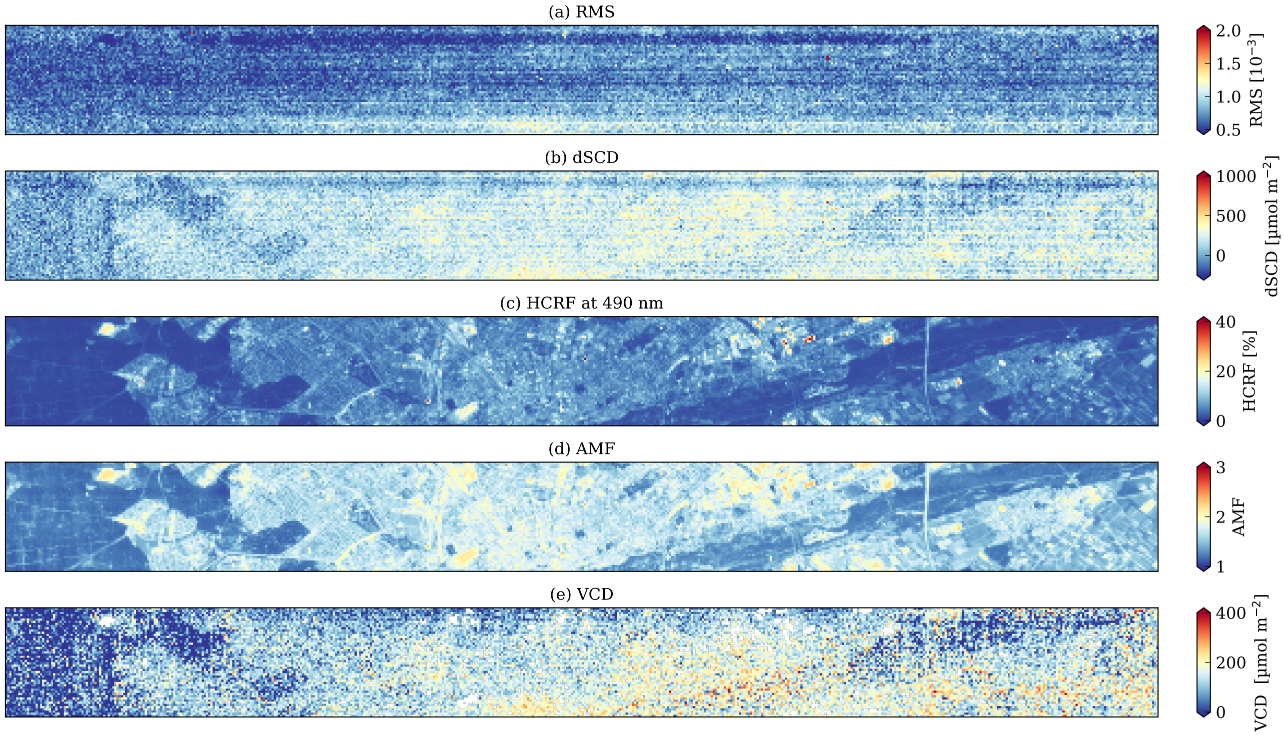


**Figure S9.** APEX stripe #3: (a) root mean square errors (RMS), (b) $NO_2$ differential slant column densities (dSCD), (c) surface reflectance, (d) air mass factors (AMF) and (e) $NO_2$ vertical column densities (VCD).

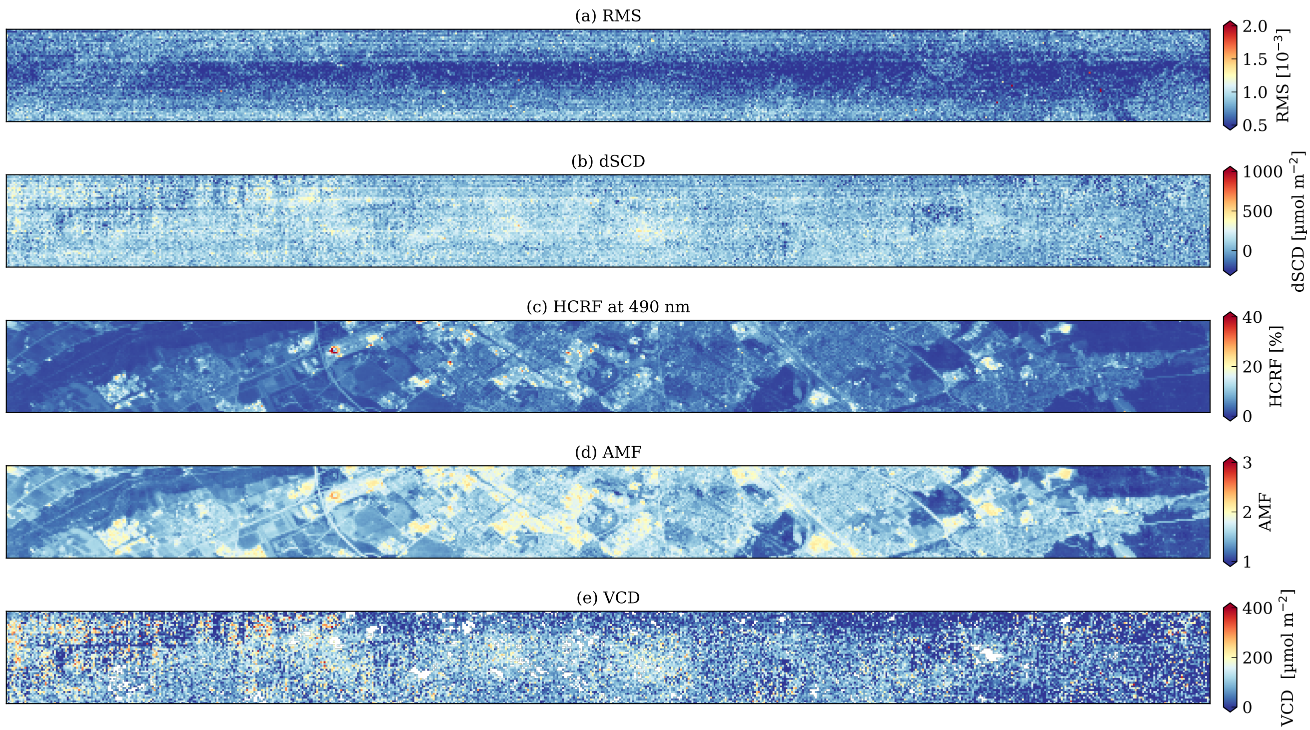


**Figure S10.** APEX stripe #4: (a) root mean square errors (RMS), (b) $NO_2$ differential slant column densities (dSCD), (c) surface reflectance, (d) air mass factors (AMF) and (e) $NO_2$ vertical column densities (VCD).

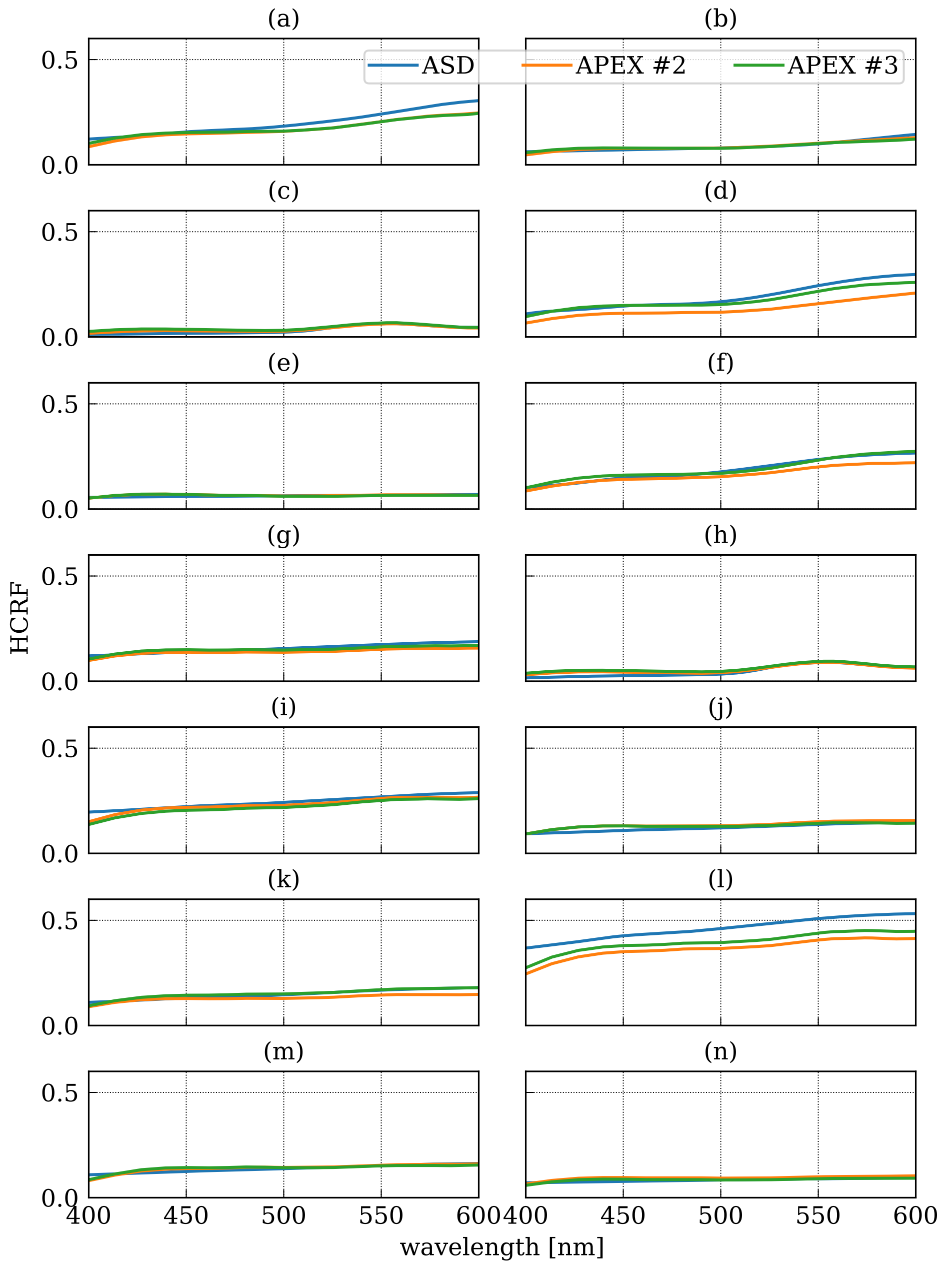


**Figure S11.** Comparison of APEX and ASD Hemispheric-conic reflectance factors (HCRF). The location of APEX and ASD measurements are shown in Table S1.

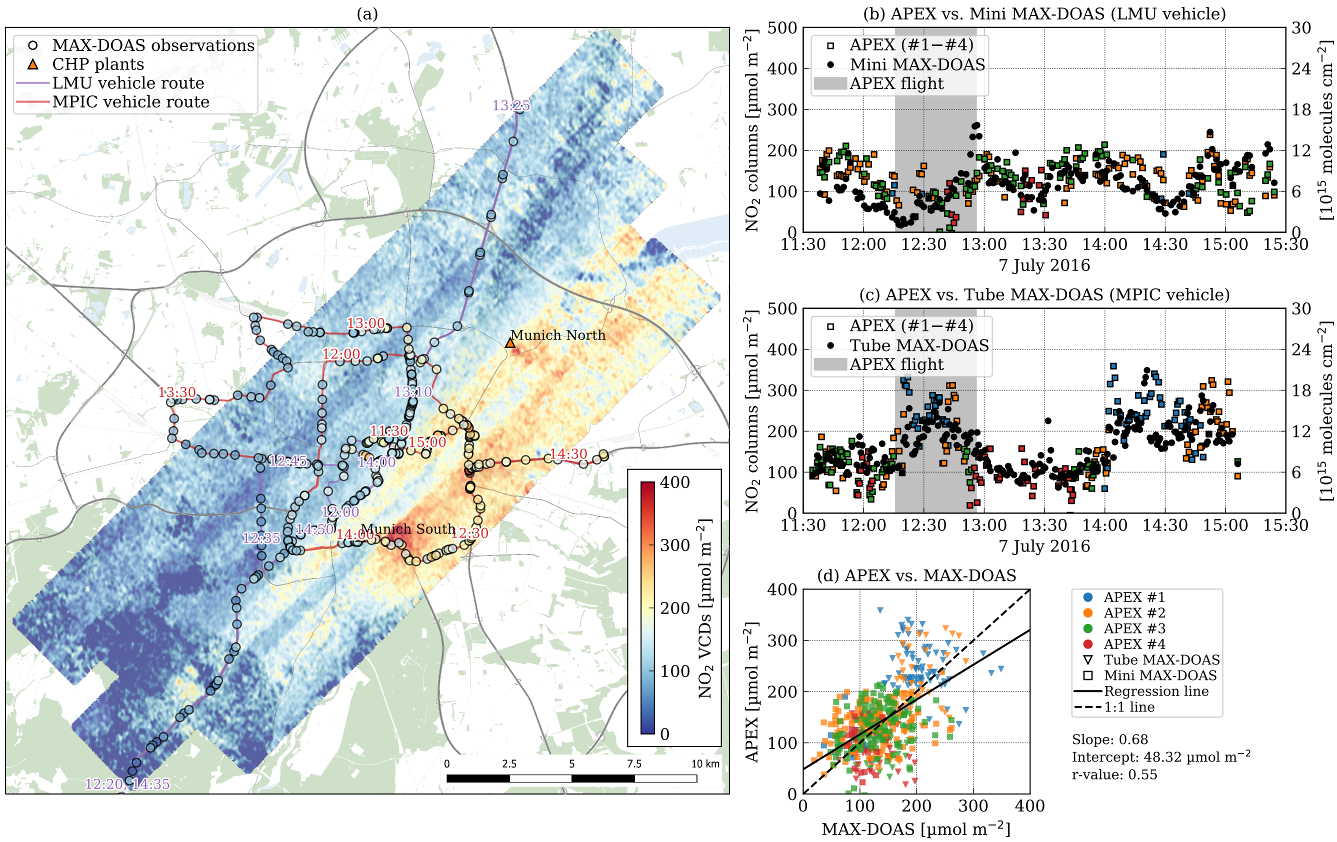


**Figure S12.** (a) Map $NO_2$ VCDs from APEX and mobile MAX-DOAS measurements on 7 July 2016 (afternoon) and time labels. (b,c) Time series of spatially co-located APEX and (b) Mini MAX-DOAS and (c) Tube MAX-DOAS VCDs. (d) Scatter plot showing MAX-DOAS and APEX $NO_2$ VCDs for spatially co-located observations. Map data from © OpenStreetMap contributors 2021. Distributed under the Open Data Commons Open Database License (ODbL) v1.0.

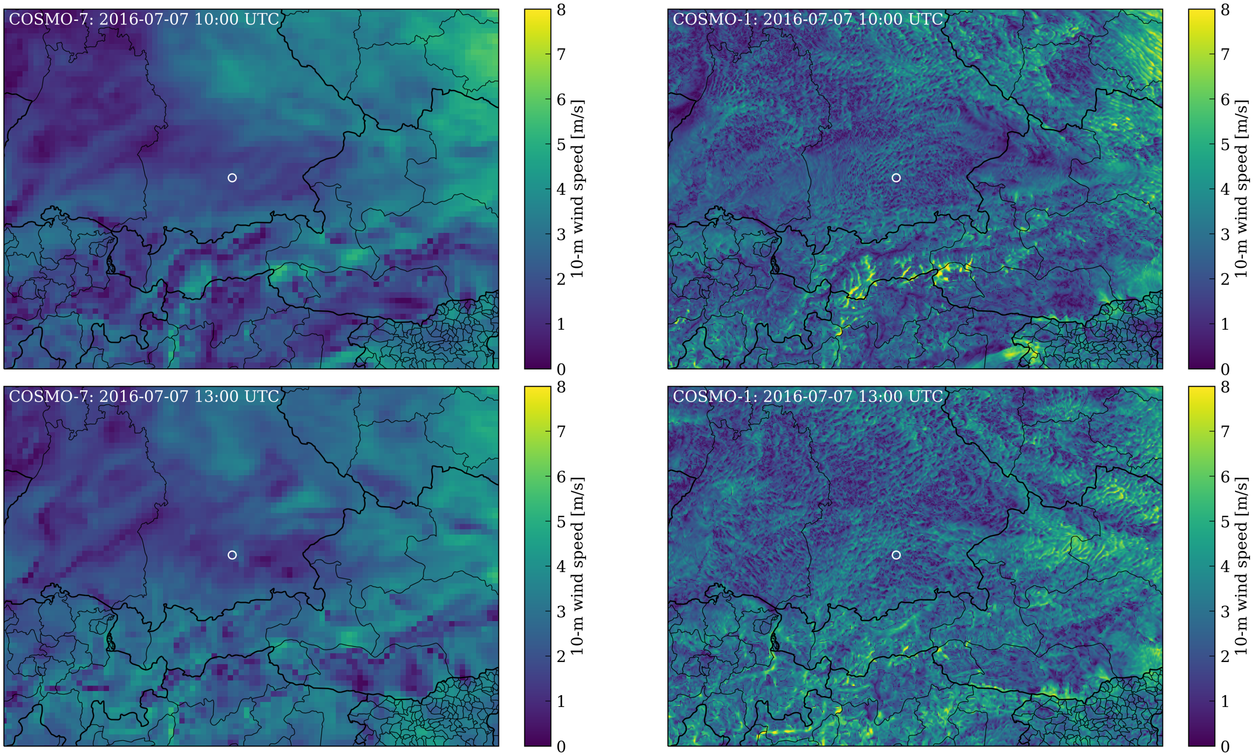


**Figure S13.** Maps of 10-m wind speeds at 10 and 13 UTC from the COSMO-7 and COSMO-1 model with 7 km and 1 km spatial resolution. The COSMO-1 model shows highly variable 10-m wind speeds over Munich with a similar spatial variability as the ground measurements. Since the COSMO-7 model does not resolve the convective cells at 7 km resolution, 10-m wind speeds vary spatially less.

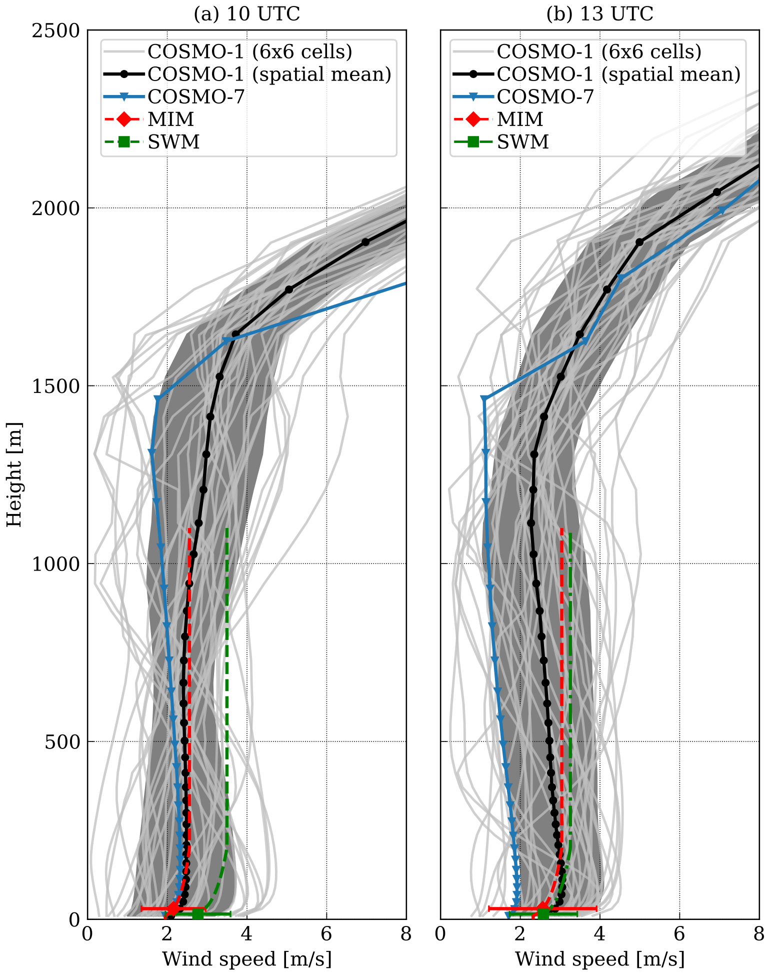


**Figure S14.** Wind profiles at (a) 10 UTC and (b) 13 UTC at Munich South CHP plant from the COSMO-1 and COSMO-7 model. COSMO-1 profiles are shown for 6×6 grid cells and as spatial mean with standard deviation. In addition, wind profiles were extrapolated from wind measurements at the MIM's rooftop and at the plant site provided by Stadtwerke München (SWM) using the empirical equations recommended by the Association of German Engineers (VDI - Fachbereich Umweltmeteorologie, 1985, 2009). At noon (10 UTC), the COSMO-1 and COSMO-7 analysis product agree quite well, but individual COSMO-1 profiles show very high variability within 6×6 grid cells. The wind profiles extrapolated from measurements also agree with the simulated wind fields. In the afternoon (13 UTC), COSMO-1 winds increased by about $1\,\mathrm{m\,s^{-1}}$, while COSMO-7 winds remain similar to the noon values.

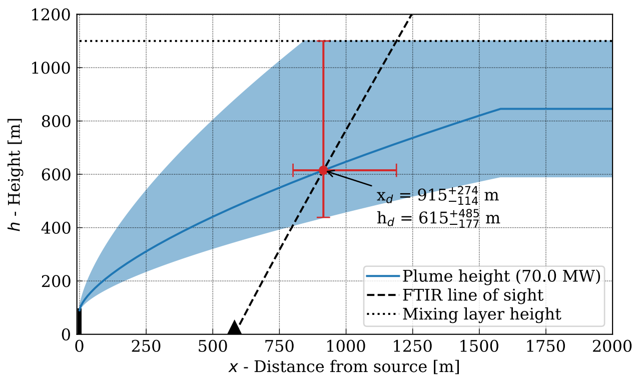


**Figure S15.** Plume rise of emission plume of Munich South CHP plant assuming heat emissions of 70 MW using VDI guidelines. The plume height and the line-of-sight of the FTIR spectrometer intersect at about $x_d = 918\,\mathrm{m}$ downstream of the source at $h_d = 620\,\mathrm{m}$ above ground. The uncertainty is obtained from the uncertainty of the wind speed at the stack ($2.5 \pm 1.2\,\mathrm{m\,s^{-1}}$).

## S2 Additional Tables

**Table S1.** Name and locations of APEX and ASD reflectance spectra. Indices in APEX stripes #2 and #3 are shown.

| # | Surface type | Location | Longitude [°E] | Latitude [°N] | APEX index (#2) across | APEX index (#2) along | APEX index (#3) across | APEX index (#3) along |
|---|---|---|---|---|---|---|---|---|
| 1 | Sand | Sports ground | 11.5245 | 48.1268 | 30 | 3373 | 381 | 1822 |
| 2 | Cinder track | Sports ground | 11.5240 | 48.1270 | 22 | 3387 | 391 | 1813 |
| 3 | Lawn | Sports ground | 11.5239 | 48.1264 | 35 | 3384 | 377 | 1811 |
| 4 | Tartan track | Westpark | 11.5398 | 48.1286 | 224 | 3174 | 187 | 1979 |
| 5 | Dark asphalt | Westpark | 11.5410 | 48.1284 | 238 | 3165 | 165 | 1985 |
| 6 | Bright gravel | Westpark | 11.5408 | 48.1283 | 243 | 3169 | 167 | 1981 |
| 7 | Bright asphalt | Theresienwiese | 11.5526 | 48.1312 | 349 | 2992 | 60 | 2123 |
| 8 | Lawn | Koenigsplatz | 11.5658 | 48.1452 | 209 | 2646 | 200 | 2460 |
| 9 | Gravel | Koenigsplatz | 11.5651 | 48.1455 | 188 | 2647 | 220 | 2460 |
| 10 | Cobblestones | Koenigsplatz | 11.5649 | 48.1460 | 169 | 2649 | 233 | 2462 |
| 11 | Bright cobblestones | Koenigsplatz | 11.5642 | 48.1463 | 155 | 2644 | 249 | 2457 |
| 12 | Bright paving stone | Koenigsplatz | 11.5674 | 48.1454 | 226 | 2623 | 186 | 2477 |
| 13 | Paving stone | LMU main building | 11.5816 | 48.1507 | 301 | 2378 | 100 | 2683 |
| 14 | Dark cobblestones | Siegestor | 11.5821 | 48.1522 | 275 | 2353 | 129 | 2711 |

**Table S2.** Input and output parameter from emission quantification of $NO_x$ emissions with distance from source $L$, effective plume height $h_d$, wind speed in plume $u$, angle between wind centerline and APEX stripe $\alpha$, residence time $\tau$, $NO_2$-to-$NO_x$ conversion factor $f$, estimated emissions $Q$ as well as standard width $\sigma$ and location $\mu$ of Gaussian curve.

| Stripe | Source | Box | $L$ [m] | $h_d$ [m] | $u$ [m s$^{-1}$] | $\alpha$ [deg] | $\tau$ [s] | $f$ | $Q$ [kg s$^{-1}$] | $\sigma$ [m] | $\mu$ [m] |
|---|---|---|---|---|---|---|---|---|---|---|---|
| #1 | M. South | 1 | 342.4 | 279.7 | 3.2±1.3 | 34±5 | 108.1 | 10.5±4.3 | 26.7±16.1 | 43±8 | -14±9 |
| #1 | M. South | 2 | 820.9 | 430.0 | 2.9±1.2 | 41±5 | 282.6 | 4.3±1.5 | 80.0±43.7 | 398±37 | -447±39 |
| #1 | M. South | 3 | 1364.3 | 567.0 | 2.7±1.0 | 49±5 | 500.4 | 2.7±0.8 | 48.9±24.3 | 374±29 | -63±36 |
| #2 | M. South | 1 | 398.4 | 306.9 | 3.0±1.3 | 46±5 | 131.0 | 8.8±3.4 | 115.9±66.2 | 240±17 | -88±22 |
| #2 | M. South | 2 | 851.4 | 450.0 | 2.8±1.1 | 38±5 | 298.9 | 4.1±1.5 | 51.6±27.9 | 154±9 | 170±10 |
| #2 | M. North | 1 | 213.2 | 232.9 | 3.5±0.9 | 1±5 | 61.4 | 18.1±4.7 | 106.7±44.0 | 190±35 | -1±33 |
| #2 | M. North | 2 | 554.1 | 360.2 | 3.5±1.0 | 6±5 | 157.7 | 7.4±2.0 | 43.2±18.0 | 131±20 | 60±19 |
| #2 | M. North | 3 | 916.7 | 468.1 | 3.6±1.2 | 12±5 | 256.8 | 4.7±1.4 | 54.6±26.3 | 460±84 | -266±73 |

**Table S3.** Input and output parameter from emission quantification of $CO_2$ emissions with differential column measurement (DCM), wind speed at stack $u_{\text{stack}}$, distance from stack $x_d$, height of plume $h_d$, wind speed inside plume $u_{\text{plume}}$, dispersion coefficient $\sigma_y$ and estimated $CO_2$ emissions $Q$.

| Peak | UTC | DCM [kg $m^{-2}$] | $u_{\text{stack}}$ [m s$^{-1}$] | $x_d$ [m] | $h_d$ [m] | $u_{\text{plume}}$ [m s$^{-1}$] | $\sigma_y$ [m] | $Q$ [kg s$^{-1}$] |
|---|---|---|---|---|---|---|---|---|
| 1 | 09:47 | 0.068 | 2.5±1.1 | $918^{+271}_{-110}$ | $621^{+463}_{-169}$ | $2.3 \pm 0.7$ | $318^{+84}_{-35}$ | $124.2 \pm 46.8$ |
| 2 | 09:48 | 0.028 | 2.5±1.1 | $918^{+271}_{-110}$ | $621^{+467}_{-169}$ | $2.3 \pm 0.7$ | $318^{+84}_{-35}$ | $51.0 \pm 23.6$ |
| 3 | 09:48 | 0.043 | 2.5±1.2 | $918^{+271}_{-110}$ | $621^{+471}_{-170}$ | $2.3 \pm 0.7$ | $318^{+84}_{-35}$ | $79.2 \pm 32.0$ |
| 4 | 09:51 | 0.035 | 2.5±1.2 | $918^{+271}_{-112}$ | $620^{+480}_{-172}$ | $2.3 \pm 0.7$ | $318^{+84}_{-35}$ | $64.9 \pm 27.8$ |
| 5 | 09:57 | 0.070 | 2.5±1.2 | $918^{+271}_{-115}$ | $620^{+480}_{-177}$ | $2.4 \pm 0.7$ | $318^{+84}_{-36}$ | $131.8 \pm 49.9$ |
| 6 | 10:00 | 0.035 | 2.5±1.3 | $918^{+271}_{-117}$ | $620^{+480}_{-179}$ | $2.4 \pm 0.7$ | $318^{+84}_{-37}$ | $67.1 \pm 28.9$ |
| 7 | 10:01 | 0.070 | 2.5±1.3 | $915^{+274}_{-114}$ | $615^{+485}_{-177}$ | $2.4 \pm 0.7$ | $317^{+85}_{-36}$ | $134.4 \pm 51.3$ |
| 8 | 10:11 | 0.049 | 2.6±1.3 | $903^{+286}_{-107}$ | $594^{+487}_{-166}$ | $2.4 \pm 0.8$ | $313^{+88}_{-34}$ | $91.0 \pm 38.2$ |
| 9 | 10:17 | 0.032 | 2.6±1.3 | $896^{+293}_{-103}$ | $581^{+454}_{-159}$ | $2.4 \pm 0.8$ | $311^{+91}_{-32}$ | $58.0 \pm 27.6$ |
| 10 | 10:28 | 0.047 | 2.7±1.3 | $884^{+305}_{-95}$ | $559^{+407}_{-149}$ | $2.3 \pm 0.9$ | $307^{+94}_{-30}$ | $85.0 \pm 39.2$ |
| 11 | 10:44 | 0.039 | 2.8±1.3 | $869^{+293}_{-87}$ | $532^{+351}_{-135}$ | $2.3 \pm 1.0$ | $302^{+91}_{-27}$ | $69.1 \pm 34.8$ |
| 12 | 10:48 | 0.045 | 2.9±1.3 | $865^{+278}_{-84}$ | $525^{+337}_{-132}$ | $2.3 \pm 1.0$ | $301^{+86}_{-27}$ | $78.7 \pm 39.2$ |
| 13 | 10:55 | 0.065 | 2.9±1.3 | $859^{+259}_{-81}$ | $514^{+318}_{-127}$ | $2.3 \pm 1.0$ | $299^{+80}_{-26}$ | $114.6 \pm 55.8$ |
| 14 | 11:09 | 0.021 | 3.1±1.3 | $844^{+216}_{-73}$ | $487^{+274}_{-115}$ | $2.5 \pm 1.1$ | $295^{+67}_{-23}$ | $37.8 \pm 22.9$ |
| 15 | 11:19 | 0.051 | 3.2±1.3 | $833^{+189}_{-67}$ | $468^{+246}_{-107}$ | $2.6 \pm 1.1$ | $291^{+59}_{-21}$ | $97.0 \pm 46.0$ |
| 16 | 11:30 | 0.030 | 3.4±1.3 | $823^{+165}_{-62}$ | $449^{+220}_{-99}$ | $2.7 \pm 1.1$ | $288^{+52}_{-20}$ | $58.7 \pm 30.1$ |
| 17 | 11:34 | 0.040 | 3.4±1.3 | $819^{+158}_{-59}$ | $443^{+212}_{-96}$ | $2.8 \pm 1.1$ | $287^{+50}_{-19}$ | $80.0 \pm 38.1$ |
| 18 | 11:47 | 0.019 | 3.6±1.3 | $809^{+138}_{-55}$ | $424^{+189}_{-89}$ | $2.9 \pm 1.2$ | $284^{+43}_{-17}$ | $38.7 \pm 23.5$ |

## References


VDI - Fachbereich Umweltmeteorologie: Dispersion of air pollutants in the atmosphere; determination of plume rise, Tech. Rep. VDI 3782 Blatt 3, VDI/DIN-Kommission Reinhaltung der Luft (KRdL) - Normenausschuss, 1985.

VDI - Fachbereich Umweltmeteorologie: Atmospheric dispersion models; Gaussian plume model for the determination of ambient air characteristics, Tech. Rep. VDI 3782 Blatt 1, VDI/DIN-Kommission Reinhaltung der Luft (KRdL) - Normenausschuss, 2009.

Zhu, Y., Chen, J., Bi, X., Kuhlmann, G., Chan, K. L., Dietrich, F., Brunner, D., Ye, S., and Wenig, M.: Spatial and temporal representativeness of point measurements for nitrogen dioxide pollution levels in cities, Atmospheric Chemistry and Physics, 20, 13 241–13 251, https://doi.org/10.5194/acp-20-13241-2020, 2020.